Journal of Materials Chemistry C

PAPER

View Article Online
View Journal | View Issue

Cite this: J. Mater. Chem. C, 2014, 2, 10195

Enhanced performance of polymer bulk heterojunction solar cells employing multifunctional iridium complexes†

Myoung Hee Yun,[a] Eung Lee,[b] Woochul Lee,[c] Hyosung Choi,[a] Bo Ram Lee,[d] Myoung Hoon Song,[d] Jong-In Hong,*[c] Tae-Hyuk Kwon*[b] and Jin Young Kim*[a]

Received 10th June 2014
Accepted 26th September 2014

DOI: 10.1039/c4tc01222d

www.rsc.org/MaterialsC

We report on the enhanced performance of polymer bulk heterojunction solar cells composed of an iridium complex with pendant sodium cations (pqIrpicNa) as an energy donor, poly(3-hexylthiophene) (P3HT) as an energy acceptor, polyethylene oxide (PEO) as an ion channel, and PCBM as an electron acceptor. With the iridium complex and PEO as additives, we observe a 20% increase in the current density, from 8.57 mA cm^{-2} to 10.24 mA cm^{-2}, and a photoconversion efficiency of up to 3.4%. The observed enhancement in current density comes primarily from an efficient triplet–singlet energy transfer from the iridium complex to P3HT. Transient photoluminescence studies reveal triplet–singlet energy transfer efficiency from pqIrpicNa to P3HT of over 99%. Because of this high energy transfer efficiency, an enhancement is observed in the incident photon-to-conversion efficiency spectrum between 350 and 550 nm, which overlaps with the absorption range of the iridium complex. We also observe enhanced nanophase segregation of the active layer with pqIrpicaNa and PEO by atomic force microscopy. We propose that the observed enhancement in the current density stems not only from the enhancement in the morphology with the iridium complex, but also from the enhanced mobility of the sodium cations toward the metal electrodes through the ion channel of PEO under sunlight, which results in an increased charge collection at the electrodes.

Introduction

Bulk heterojunction (BHJ) solar cells consisting of an electron donor and an electron acceptor are an attractive type of solar cell because they are inexpensive, simple to process, lightweight, and flexible.[1–7] The most common donor material in BHJ solar cells is regioregular poly(3-hexylthiophene) (P3HT), using which, it is possible to achieve a photoconversion efficiency (PCE) greater than 6%.[8] Despite their many promising advantages, the highest photovoltaic efficiency reported for BHJ solar cells to date is less than 10%,[9] which is significantly less than the value predicted by modeling (15%).[10] There are many factors limiting the performance of BHJ solar cells, such as the optical absorbance, purity of the polymer materials, exciton diffusion length, charge separation, and charge collection at the electrode. In addition, the morphology of the active composite layer has an impact on the photovoltaic performance, and the energy barrier between electrodes and the active layer can intrinsically limit the current density as well. Among these factors, one of the major challenges in BHJ solar cells is to fabricate devices that can efficiently absorb sunlight from the visible to the near IR region (350–900 nm), as it is very difficult to obtain a wide absorption range and a high extinction coefficient using a single material. Energy transfer between an energy donor and an acceptor with different absorption spectra could be an ideal strategy to solve this issue.

Energy transfer has been widely employed to enhance both the signal-to-noise ratio in biosensors[11,12] and the efficiency of organic light-emitting diodes (OLEDs).[13] The criteria for an energy donor capable of efficient energy transfer are high quantum efficiency, efficient overlap between the absorption spectrum of the energy acceptor and the emission spectrum of the energy donor, minima overlap with the absorption range of the energy acceptor, a large Stokes shift to prevent self-quenching, and a higher energy gap than that of the energy acceptor to prevent charge transfer. There are three types of energy transfer: singlet–singlet energy transfer, which is known

[a]School of Energy and Chemical Engineering, Ulsan National Institute of Science and Technology (UNIST), Ulsan, 689-798, Korea. E-mail: jykim@unist.ac.kr
[b]Department of Chemistry, Ulsan National Institute of Science and Technology (UNIST), Ulsan, 689-798, Korea. E-mail: kwon90@unist.ac.kr
[c]Department of Chemistry, Seoul National University, Seoul 151–747, Korea. E-mail: jihong@snu.ac.kr
[d]School of Materials Science and Engineering and KIST-UNIST Ulsan Center for Convergent Materials, Ulsan National Institute Science and Technology (UNIST), Ulsan, 689-798, Korea

† Electronic supplementary information (ESI) available: Emission spectrum of P3HT and PCBM with pqIrpicNa, IPCE data of pqIrpicNa:PCBM, ΔIPCE of P3HT:PCBM, table of exciton lifetime, and other AFM images. See DOI: 10.1039/c4tc01222d

as Förster resonance energy transfer (FRET),[14] triplet–triplet energy transfer, which is known as Dexter energy transfer,[15] and triplet–singlet energy transfer, which is similar to FRET.[16,17] Dexter energy transfer, employing triplet excitation with iridium complexes, plays an important role in increasing the efficiency of OLEDs. This is because iridium complexes have a high quantum efficiency, a large Stokes shift, and a long exciton diffusion length. The long diffusion length present in iridium complexes is very beneficial in BHJ solar cells because the diffusion length of singlet excitons in most photovoltaic materials is usually between 5 and 10 nm,[18,19] which is much shorter than that required for efficient light absorption.

Iridium complexes have been studied in organic BHJ solar cells as electron donor materials but have failed to attain reasonable efficiencies due to their low hole mobilities.[20] Alternatively, iridium complexes have been implemented in BHJ solar cells as dopants to increase the triplet population, thereby increasing the photoconversion efficiency,[21–23] or as an additive to improve the morphology.[24] Although triplet states have a long diffusion length, there are few reports on the enhanced performance of BHJ solar cells using energy transfer with a triplet excited state except for those operating by the FRET mechanism. Recently, the Taylor group demonstrated that FRET significantly improved the light absorption and PCE for BHJ solar cells.[25] Therefore, because triplet states have a longer diffusion length than singlet states, employing triplet energy transfer is a promising strategy for the fabrication of BHJ solar cells.

In this research, we suggest a novel approach to fabricating a BHJ solar cell that involves a multifunctional iridium complex containing pendant Na^+ ions (pqIrpicNa) as an energy donor, P3HT as an energy acceptor, Phenyl-C61-butyric acid methyl (PCBM) as an electron acceptor, and polyethylene oxide (PEO) as an ion channel to improve the ionic mobility[26,27] and morphology control.[28] The most promising advantages of pqIrpicNa are that its absorption range exhibits a small overlap with that of the energy acceptor, a large Stokes shift, and a reasonable quantum efficiency. The transient photoluminescence (PL) spectrum, measured by time-correlated single photon counting (TCSPC), showed energy transfer efficiencies of over 99% from pqIrpicNa to P3HT. Furthermore, recent research showed that ionic iridium complexes enhanced the phase separation between the donor and the acceptor, leading to an increase in the photovoltaic performance.[24] Overall, the extent of the phase separation is influenced by the hydrophobicity of the iridium complex, which can be controlled by varying the ligands. Therefore, the neutral iridium complex (pqIrpicNa) with a hydrophobic unit, 2-phenylquinoline (pq), can offer great potential to improve the morphology. The sodium ion of pqIrpicNa is generally known to have a faster mobility in the solid film with PEO. Thus, Na^+ is expected to reduce the energy barrier between the electrode and the organic material by moving the cation toward the electrode[29] when the electric field is formed by sunlight, increasing the exciton diffusion length by stabilizing the exciton. In this manner, charge collection at the electrodes is improved. To demonstrate the various advantages of iridium complexes mentioned above, we evaluated BHJ solar cells containing various amounts of pqIrpicNa to demonstrate the energy transfer effect between the Ir complex and P3HT, to envisage the ion channel effect of the Na^+ ion with or without PEO, and to control the morphology of the active layer. The presence of pqIrpicNa improved the photocurrent (J_{SC}) in the BHJ solar cells and the morphology. As a result, the overall photoconversion efficiency of P3HT:PCBM solar cells is improved from 3.0% to 3.4%.

Experimental

The synthesis of pqIrpicNa was carried out using a previously reported procedure.[29] Optimized BHJ devices were prepared as follows. Indium tin oxide (ITO)-coated glass substrates were cleaned with distilled water, then sonicated in distilled water, acetone, and isopropyl alcohol, and dried overnight in an oven. Next, an aqueous solution of poly(3,4-ethylenedioxythiophene):poly(styrenesulfonate) (PEDOT:PSS) was spun-cast to form a film with a thickness of approximately 40 nm. The films were annealed for 10 min at 140 °C in air and then transferred to a nitrogen-filled glovebox. Next, active layers were deposited from a mixture of 2 wt% P3HT : PCBM (1 : 0.8 w/w) in *o*-dichlorobenzene without and with varying ratios of the Ir complex and PEO (1 : 0, 3 : 1, 1 : 1, 1 : 3, and 0 : 1 wt% relative to the P3HT concentration). The devices were completed by the thermal evaporation of Al cathodes (~100 nm) at a base pressure of 10^{-6} Torr. Device characterization was carried out in a nitrogen-filled glovebox by recording the current density–voltage (*J*–*V*) curves with a Keithley 2635 A source measurement unit under simulated AM1.5G radiation (calibrated to 100 mW cm^{-2}) using a high quality optical fiber coupled to a xenon arc lamp. Atomic force microscopy (AFM) images were obtained using a Veeco microscope in tapping mode over a 1 μm × 1 μm scan area. The exciton lifetime was determined by a TCSPC technique. The details can be found in a previous report.[30]

Results and discussion

Photophysical properties and energy transfer

The molecular structures and photophysical properties of the materials used in this research are shown in Fig. 1a. The synthesis of pqIrpicNa followed a previously published method. The emission spectrum of pqIrpicNa efficiently overlaps with the absorption spectrum of P3HT, as shown in Fig. 1b. The absorption range of pqIrpicNa below 450 nm does not inhibit the absorption of P3HT, and pqIrpicNa has never been used in devices outside of being an energy donor.

The highest occupied molecular orbital (HOMO) energy of pqIrpicNa (−5.6 eV) is lower than that of P3HT (−5.1 eV), and the lowest unoccupied molecular orbital (LUMO) energy of pqIrpicNa (−2.9 eV) is higher than that of P3HT (−3.0 eV), which allows for efficient energy transfer (not charge transfer) from pqIrpicNa to P3HT (Fig. 2). To confirm the energy transfer from pqIrpicNa to P3HT, both the steady-state photoluminescence (PL) and transient PL were measured by TCSPC.[31] First, we compared the PL intensity of P3HT containing 1 wt%

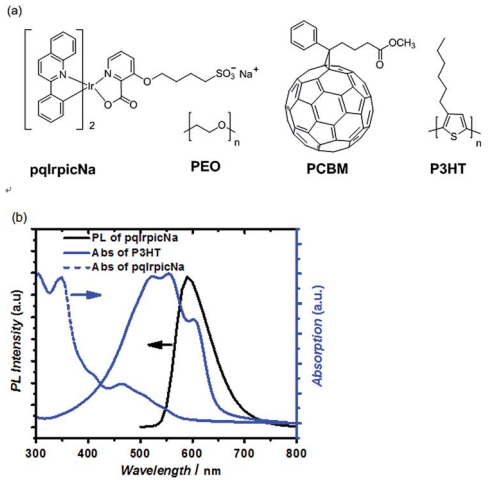

Fig. 1 (a) Chemical structures of P3HT, PCBM, pqIrpicNa, and PEO. (b) Photoluminescence spectrum of the energy donor (black line: pqIrpicNa) and absorption spectra of the energy acceptor and donor (blue solid line: P3HT, blue dashed line: pqIrpicNa).

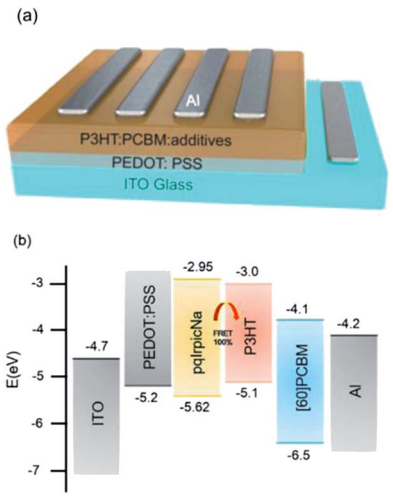

Fig. 2 (a) Device structure and (b) band diagram of ITO, PEDOT:PSS, pqIrpicNa, P3HT, PCBM, and Al.

pqIrpicNa with that of pure P3HT when it was excited in the metal-to-ligand charge transfer (MLCT) region of pqIrpicNa (470 nm) in a solid film (Fig. S1†). The PL intensity of P3HT with pqIrpicNa slightly increased and exhibited no emission from pqIrpicNa (~600 nm). Therefore, the PL intensity enhancement was derived from the energy transfer from pqIrpicNa to P3HT. We carried out transient PL measurements to more precisely evaluate the energy transfer efficiency, E, which can be calculated using the following formula:[31,32]

$$\text{ET efficiency (\%)} = (1 - \tau_{D-A}/\tau_D) \times 100, \quad (1)$$

where τ_{D-A} and τ_D are the excited state lifetimes of the energy donor (pqIrpicNa) with and without the energy acceptor (P3HT), respectively. In solid films, the lifetime for pristine pqIrpicNa was 0.3 μs, while the lifetime for pqIrpicNa with P3HT

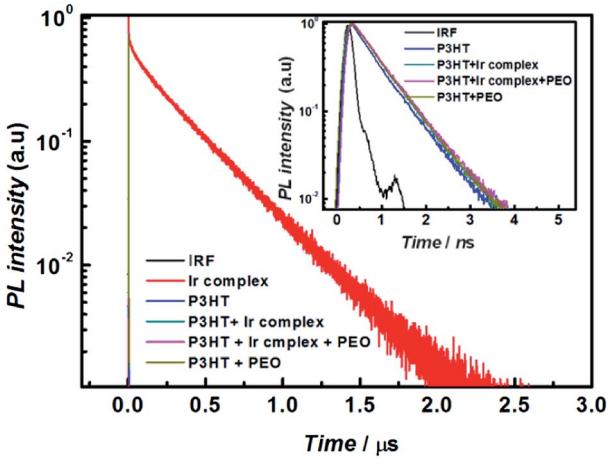

Fig. 3 Time-resolved PL signal at 600 nm of pqIrpicNa ($\lambda_{ex} = 470$ nm) with and without P3HT and/or PEO measured by time-correlated single photon counting (TCSPC) (the inset shows the time-resolved PL signal of P3HT with and/or without pqIrpicNa and/or PEO).

dramatically decreased to 0.5 ns when excited at 470 nm, which corresponds to 99.8% energy transfer efficiency (E), as shown in Fig. 3 and Table S1.† A decrease in the lifetime of the energy donor is a very typical phenomenon with efficient energy transfer.[31] The inset of Fig. 3 also demonstrates a change in the lifetime of P3HT with pqIrpicNa. There are no significant changes in the lifetime of P3HT with and without the energy donor, because the rate of energy transfer is similar to or faster than the lifetime of pristine P3HT.

BHJ solar cell studies

We fabricated solar cell devices with various concentrations (wt%) of pqIrpicNa as an energy donor and PEO as an ion channel, *i.e.*, 1 : 0, 3 : 1, 1 : 1, 1 : 3, and 0 : 1 pqIrpicNa : PEO. The structure of the devices is shown in Fig. 2. For these fabricated devices, the J–V characteristics under AM1.5G

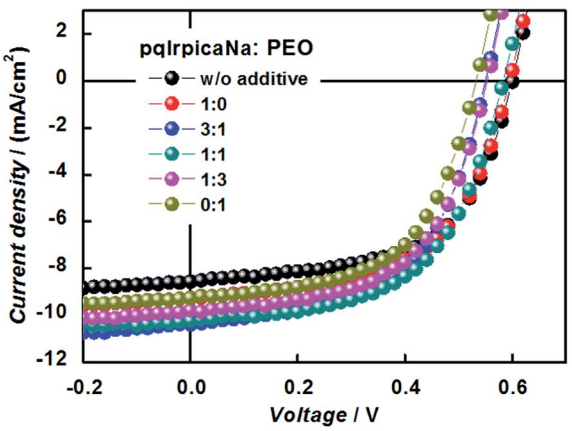

Fig. 4 Current density–voltage (J–V) characteristics of the P3HT:PCBM devices with different ratios of pqIrpicaNa to PEO measured under AM1.5G illumination from a calibrated solar simulator with an irradiation intensity of 100 mW cm^{-2}.

Table 1 Photovoltaic parameters of the P3HT:PCBM device with different ratios of additives

Active layer	pqIrpicNa : PEO	Thermal annealing (°C)	J_{SC} (mA cm^{-2})	V_{OC} (V)	FF	Efficiency (%)
P3HT : PCBM (1 : 0.8)	×	×	6.31	0.51	0.50	1.6
		150	8.57	0.60	0.59	3.0
	1 : 0	×	4.39	0.46	0.43	0.9
		150	9.27	0.60	0.57	3.1
	3 : 1	×	7.45	0.54	0.54	2.2
		150	10.40	0.55	0.56	3.2
	1 : 1	×	7.40	0.59	0.44	1.9
		150	10.24	0.58	0.56	3.4
	1 : 3	×	8.06	0.54	0.56	2.4
		150	9.79	0.55	0.57	3.1
	0 : 1	×	8.40	0.54	0.58	2.6
		150	9.26	0.53	0.57	2.8

illumination (100 mW cm^{-2}) are shown in Fig. 4 and summarized in Table 1. The reference P3HT:PCBM device exhibited a short-circuit current density (J_{SC}) of 8.57 mA cm^{-2}, an open circuit voltage (V_{OC}) of 0.60 V, and a fill factor (FF) of 0.59, which corresponds to a 3.0% PCE. The J_{SC} of the BHJ solar cells increased by approximately 20% as the content of pqIrpicNa increased from 0 to 3 wt% and reached 10.40 mA cm^{-2}. With PEO, the J_{SC} also improved from 9.27 to 10.24 mA cm^{-2} moving from a 1 : 0 to a 1 : 1 ratio of pqIrpicNa to PEO. The optimized device performance was obtained with a 1 : 1 ratio of pqIrpicNa to PEO and exhibited a 10% enhancement compared to the reference device, which corresponded to a 3.4% PCE with a J_{SC} of 10.2 mA cm^{-2}, a V_{OC} of 0.58 V, and a FF of 0.56. This enhancement of the photovoltaic performance could be attributed to the triplet–singlet energy transfer, ion channel effect, and morphology enhancement. We obtained evidence of the triplet–singlet energy transfer by the incident photon-to-current efficiency (IPCE), which is in accordance with the J_{SC} of the devices, as shown in Fig. 5. When 1 wt% pqIrpicNa was added without PEO, an IPCE enhancement was observed from 350–450 nm, which corresponds exactly to the MLCT region of pqIrpicNa and the IPCE spectrum of pqIrpicNa and PCBM (Fig. 5 and S2†). Thus, we assume that the enhancement was derived from the triplet–singlet energy transfer. The IPCE over 450 nm was slightly increased, which might be derived from an enhancement in the morphology and/or triplet–singlet energy transfer. An enhancement in the IPCE spectrum from 450 nm to 600 nm was also observed when PEO as an ion channel was added to the active layer (Fig. 5).

In Fig. 6, we put forth a plausible mechanism for the ion channel effects on the J_{SC} enhancement over 450 nm. First, the photoexcited material forms an exciton. This exciton can then be stabilized by being surrounded with Na^+ ions and Ir–SO_3^- ions (Process 1), increasing the lifetime and diffusion length of the excitons, as well as decreasing their self-recombination rate.[33] In the following step, the excitons migrate to the donor–acceptor interface and dissociate into charge carrier holes in the donor and electrons in the acceptor, and then they move to the electrodes. The sum of these processes produces a potential between the ITO and the metal electrode (Process 2). Once this potential is formed, small Na^+ ions rapidly move towards the Al electrode through the PEO ion channel, while the bulky Ir–SO_3^-

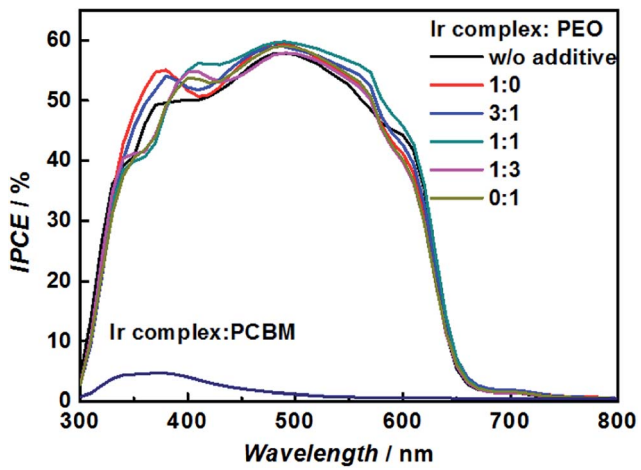

Fig. 5 IPCE data of the P3HT:PCBM devices with different ratios of additives.

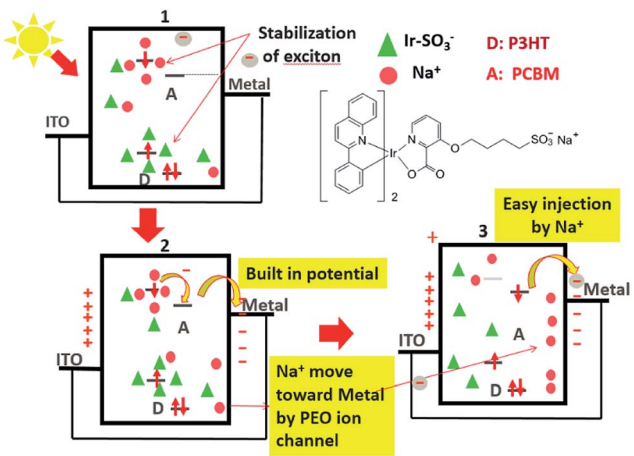

Fig. 6 Plausible mechanism of the PEO ion channel in P3HT and PCBM with pqIrpicNa and PEO.

ions remain at the counter electrode.[29] The accumulated Na^+ ions at the metal electrode can reduce the energy barrier between the metal and the active layer, which is very similar to the way in which light-emitting electrochemical cells function at a low operating voltage (Process 3). The decreased energy barrier between the metal electrode and the active layer consequently increases the current density, resulting in an enhancement of the IPCE over 450 nm.

Changes in the morphology can also enhance the IPCE over 450 nm. AFM images were collected to evaluate the effect of pqIrpicNa and PEO on the phase separation of P3HT:PCBM composite films according to their ratios (Fig. 7 and S3†). All of the films were thermally annealed at 150 °C for 5 min.[34] The morphology of the pristine P3HT:PCBM film shows (Fig. 7a) a somewhat rough surface compared to the composite films containing pqIrpicNa and/or PEO (Fig. 7b and S3†). The root mean square (RMS) roughness of the P3HT:PCBM film (3.87) was reduced to 0.42 with a 1 : 1 ratio of pqIrpicNa to PEO (Fig. 7b), 0.63 with pqIrpicNa (Fig. S3a†), and 0.55 with PEO (Fig. S3d†);[35–37] the films with a 3 : 1 or 1 : 3 ratio of pqIrpicNa to PEO exhibited similar RMS roughnesses of 0.62 and 0.54, respectively (Fig. S3†). From the AFM results, it is clear that pqIrpicNa and PEO improved the nanophase segregation and compatibility of P3HT and PCBM.

The amount of added PEO was found to influence the device performance; the addition of more than 1 wt% PEO leads to a reduction in the V_{OC} (Table 1). This can be explained by the following relationship between V_{OC} and J_{SC}. The V_{OC} depends on the saturation current density (J_0), and J_{SC} can be calculated using eqn (2).[38]

$$V_{OC} = \frac{nkT}{q} \ln\left(\frac{J_{SC}}{J_0} + 1\right), \quad (2)$$

where q is the charge of an electron, n is the ideality factor, k is the Boltzmann constant, and T is the temperature. While J_{SC} typically varies only slightly, the saturation current density plays a key role in the V_{OC} because it varies by orders of magnitude.

To attain a high V_{OC}, J_0 must be very low, because the leakage current reduces the V_{OC}. The diode saturation current density (J_0) is extracted from the intercept on the vertical axis from the log current–voltage graph. Fig. 8 shows the J–V characteristics of the solar cells with different ratios of pqIrpicNa to PEO (0 : 0, 1 : 0, 3 : 1, 1 : 1, 1 : 3, and 0 : 1) under dark conditions. The addition of PEO without the iridium complex achieved the highest J_0 and the lowest V_{OC} (0.53 V), while the reference device without any additives exhibited a V_{OC} of 0.60 V (Table 1). The V_{OC} value with 1 wt% pqIrpicNa decreased from 0.60 V to 0.55 V as the amount of PEO increased from 0 to 3 wt%. The increase in the saturation current density corresponds to the amount of PEO in the device. Therefore, the amount of PEO should be minimized. As a result, we found that the optimal ratio of PEO to pqIrpicNa is 1 : 1, which gives a V_{OC} of 0.59 V and a higher J_{SC} than the reference device.

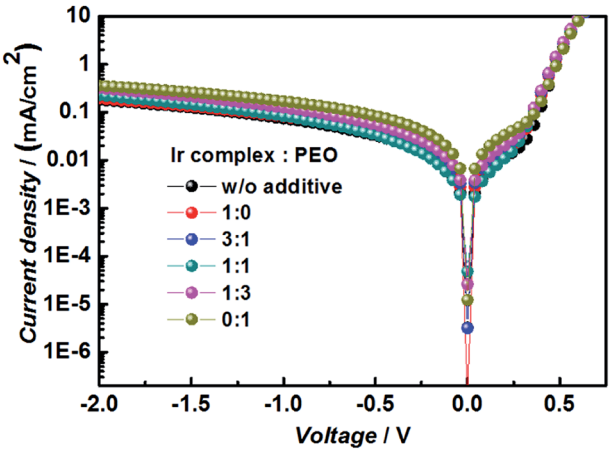

Fig. 8 Current density–voltage (J–V) characteristics in the dark of the P3HT:PCBM devices with different ratios of additives.

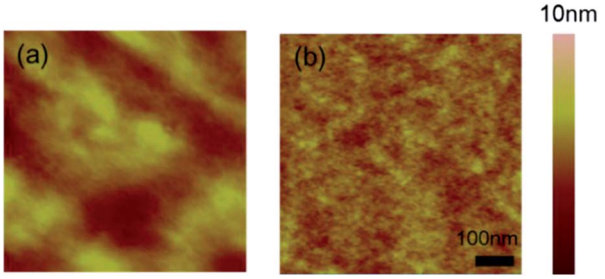

Fig. 7 AFM height images of P3HT and PCBM (a) without and (b) with a 1 : 1 ratio of pqIrpicNa : PEO.

Conclusions

In conclusion, a small amount of added pqIrpicNa and PEO enhanced the performance of BHJ solar cells because of their multifunctional abilities. Specifically, they have the ability to function as an energy donor, reduce the energy barrier between the active layer and the metal electrodes by the movement of sodium cations, and improve the morphology. The optimal ratio of pqIrpicNa to PEO was experimentally determined to be 1 : 1 in the solar cell devices, resulting in 20% and 10% increases in the J_{SC} and PCE, respectively, compared to the reference device without additives. The triplet–singlet energy transfer efficiency from pqIrpicNa to P3HT reaches 99%, which enhances the IPCE, *i.e.*, the MLCT absorption region of pqIrpicNa between 350 and 450 nm. Addition of pqIrpicNa and PEO resulted in an increase in the nanophase segregation and mobility of sodium cations through the PEO ion channels, which allow for easy collection at the electrodes. Overall, this study demonstrates that carefully chosen additives in BHJ solar cells give more control over the morphology and diffusion length within the cells, resulting in devices with improved characteristics.

Acknowledgements

This work was made possible by support from the research fund of the Ulsan National Institute of Science and Technology

(1.130073.01, 1.120017.01, and 1.120046.01), the National Research Foundation of Korea Grant (NRF-2009-0093020, NRF-2013R1A2A2A01015342, and NRF2013R1A1A2010877), and the BK21 Plus funded by the Ministry of Education, Korea (10Z20130011057). This work was also supported by a grant from the New & Renewable Energy Technology Development Program of the KETEP (no. 20113020010070), funded by the Ministry of Knowledge Economy.

Notes and references

1 G. Yu, J. Gao, J. C. Hummelen, F. Wudl and A. J. Heeger, *Science*, 1995, **270**, 1789–1791.
2 J. L. Bredas, J. E. Norton, J. Cornil and V. Coropceanu, *Acc. Chem. Res.*, 2009, **42**, 1691–1699.
3 J. Peet, A. J. Heeger and G. C. Bazan, *Acc. Chem. Res.*, 2009, **42**, 1700–1708.
4 J. W. Chen and Y. Cao, *Acc. Chem. Res.*, 2009, **42**, 1709–1718.
5 J. Roncali, *Acc. Chem. Res.*, 2009, **42**, 1719–1730.
6 Y. Y. Liang, Z. Xu, J. B. Xia, S. T. Tsai, Y. Wu, G. Li, C. Ray and L. P. Yu, *Adv. Mater.*, 2010, **22**, E135–E138.
7 B. Walker, A. B. Tomayo, X.-D. Dang, P. Zalar, J. H. Seo, A. Garcia, M. Tantiwiwat and T.-Q. Nguyen, *Adv. Funct. Mater.*, 2009, **19**, 3063–3069.
8 G. J. Zhao, Y. J. He and Y. F. Li, *Adv. Mater.*, 2010, **22**, 4355–4358.
9 S. H. Liao, H. J. Jhuo, Y. S. Cheng and S. A. Chen, *Adv. Mater.*, 2013, **25**, 4766–4771.
10 G. Dennler, M. C. Scharber, T. Ameri, P. Denk, K. Forberich, C. Waldauf and C. J. Brabec, *Adv. Mater.*, 2008, **20**, 579–583.
11 T.-H. Kwon, J. Kwon and J.-I. Hong, *J. Am. Chem. Soc.*, 2008, **130**, 3726–3727.
12 T.-H. Kwon, H. J. Kim and J.-I. Hong, *Chem.–Eur. J.*, 2008, **14**, 9613–9619.
13 C. W. Tang, S. A. Vanslyke and C. H. Chen, *J. Appl. Phys.*, 1989, **65**, 3610–3616.
14 T. Forster, *Discuss. Faraday Soc.*, 1959, 7–17.
15 D. L. Dexter, *J. Chem. Phys.*, 1953, **21**, 836–850.
16 W. C. Galley and L. Stryer, *Biochemistry*, 1969, **8**, 1831–1838.
17 S. Blumstengel, E. Colabella, A. Borghesi, R. Tubino, M. Jandke and P. Strohriegl, *Synth. Met.*, 2001, **121**, 1711–1712.
18 J. J. M. Halls, K. Pichler, R. H. Friend, S. C. Moratti and A. B. Holmes, *Appl. Phys. Lett.*, 1996, **68**, 3120–3122.
19 D. E. Markov, C. Tanase, P. W. M. Blom and J. Wildeman, *Phys. Rev. B: Condens. Matter Mater. Phys.*, 2005, **72**, 045217.
20 W. Lee, T.-H. Kwon, J. Kwon, J. Kim, C. Lee and J.-I. Hong, *New J. Chem.*, 2011, **35**, 2557.
21 C.-M. Yang, C.-H. Wu, H.-H. Liao, K.-Y. Lai, H.-P. Cheng, S.-F. Horng, H.-F. Meng and J.-T. Shy, *Appl. Phys. Lett.*, 2007, **90**, 133509.
22 F. Guo, Y.-G. Kim, J. R. Reynolds and K. S. Schanze, *Chem. Commun.*, 2006, 1887–1889.
23 Z. Xu, B. Hu and J. Howe, *J. Appl. Phys.*, 2008, **103**, 043909.
24 C. S. Kim, L. L. Tinker, B. F. DiSalle, E. D. Gomez, S. Lee, S. Bernhard and Y.-L. Loo, *Adv. Mater.*, 2009, **21**, 3110–3115.
25 J.-S. Huang, T. Goh, X. Li, M. Y. Sfeir, E. A. Bielinski, S. Tomasulo, M. L. Lee, N. Hazari and A. D. Taylor, *Nat. Photonics*, 2013, **7**, 479–485.
26 T.-W. Lee, H.-C. Lee and O. O. Park, *Appl. Phys. Lett.*, 2002, **81**, 214–216.
27 Y. Cao, G. Yu, A. J. Heeger and C. Y. Yang, *Appl. Phys. Lett.*, 1996, **68**, 3218–3220.
28 Y. Shi, F. Li and Y. Chen, *New J. Chem.*, 2013, **37**, 236–244.
29 T.-H. Kwon, Y. H. Oh, I.-S. Shin and J.-I. Hong, *Adv. Funct. Mater.*, 2009, **19**, 711–717.
30 B. R. Lee, J.-W. Kim, D. Kang, D. W. Lee, S.-J. Ko, H. J. Lee, C.-L. Lee, J. Y. Kim, H. S. Shin and M. H. Song, *ACS Nano*, 2012, **6**, 2984–2991.
31 T.-H. Kwon, M. K. Kim, J. Kwon, D.-Y. Shin, S. J. Park, C. L. Lee, J. J. Kim and J.-I. Hong, *Chem. Mater.*, 2007, **19**, 3673–3680.
32 J. R. Lakowicz, *Principles of Fluorescence Spectroscopy*, Springer, New York, 2006.
33 F. C. Chen, Q. F. Xu and Y. Yang, *Appl. Phys. Lett.*, 2004, **84**, 3181–3183.
34 X. Yang, J. Loos, S. C. Veenstra, W. J. H. Verhees, M. M. Wienk, J. M. Kroon, M. A. J. Michels and R. A. J. Janssen, *Nano Lett.*, 2005, **5**, 579–583.
35 K.-G. Lim, M.-R. Choi, H.-B. Kim, J. H. Park and T.-W. Lee, *J. Mater. Chem.*, 2012, **22**, 25148–25153.
36 F. Zhang, M. Ceder and O. Inganas, *Adv. Mater.*, 2007, **19**, 1835–1838.
37 The reduced RMS roughness might be related to the preferential location of PEO on the top surface due to phase separation, which may enhance the electron extraction.
38 S. M. Sze, *Physics of Semiconductor Devices*, Wiley, New York, 1981.

